



Accelerated Degradation Protocols for Iridium-Based Oxygen Evolving Catalysts in Water Splitting Devices

Camillo Spöri,^{1b} Cornelius Brand, Matthias Kroschel,^{1b} and Peter Strasser^{*z}^{1b}

TU Berlin, The Electrochemical Energy, Catalysis and Materials Science Laboratory, 10623 Berlin, Germany

Hydrogen production by proton exchange membrane (PEM) water electrolysis is among the promising energy storage solutions to buffer an increasingly volatile power grid employing significant amounts of renewable energies. In PEM electrolysis research, 24 h galvanostatic measurements are the most common initial stability screenings and up to 5,000 h are used to assess extended stability, while commercial stack runtimes are within the 20,000–50,000 h range. In order to obtain stability data representative of commercial lifetimes with significantly reduced test duration an accelerated degradation test (ADT) was suggested by our group earlier. Here, we present a study on the broad applicability of the suggested ADT in RDE and CCM measurements and showcase the advantage of *transient* over *static* operation for enhanced catalyst degradation studies. The suggested ADT-1.6 V protocol allows unprecedented, reproducible and quick assessment of anode catalyst long-term stability, which will strongly enhance degradation research and reliability. Furthermore, this protocol allows to bridge the gap between more fundamental RDE and commercially relevant CCM studies.

© 2021 The Author(s). Published on behalf of The Electrochemical Society by IOP Publishing Limited. This is an open access article distributed under the terms of the Creative Commons Attribution 4.0 License (CC BY, <http://creativecommons.org/licenses/by/4.0/>), which permits unrestricted reuse of the work in any medium, provided the original work is properly cited. [DOI: 10.1149/1945-7111/abeb61]



Manuscript submitted September 30, 2020; revised manuscript received February 21, 2021. Published March 11, 2021. *This paper is part of the JES Focus Issue on Proton Exchange Membrane Fuel Cell and Proton Exchange Membrane Water Electrolyzer Durability.*

Supplementary material for this article is available [online](#)

The development of general test protocols for the Oxygen Evolution Reaction (OER) and, in particular, for degradation screening of OER catalysts is of crucial importance for the success of water electrolysis and other industrial electrochemical processes that make use of the OER. Recent research has adapted to this challenge and different approaches were tested. 24 h galvanostatic measurements are the most common initial stability screenings in PEM single cell or stack tests, while runtimes up to 5,000 h are used to assess extended stability in academic research.¹ RDE-stability protocols vary largely, while commercial stack runtimes are within the 20,000–50,000 h range.² In order to obtain representative stability data with significantly reduced test duration a repetitive square-wave voltammetry protocol was designed to mimic similar PEM electrolyzer degradation effects observed by in situ ICP-MS measurement.² Alia et al. investigated the influence of chronoamperometric (CA, *static*) measurements at a set of increasing limit potentials (E_{up}) vs that of fast potential cycling between 1.4 V_{RHE} and E_{up} (CV, *transient*).³ The authors found an increased Ir degradation for static CA operation over the transient potential cycling in RDE tests of Ir nanoparticles. Regardless, they reverted to transient potential cycling on their MEA stability tests.⁴ Rakousky et al. studied the impact of current cycling (*transient*) and constant current (*static*) operation on catalyst degradation in PEM water electrolysis.⁵ They determined that high static current densities (2 A cm^{-2} , corresponding to ca. 1.9 V_{RHE} in their study) resulted in the largest performance losses. Additionally, a positive influence of current cycling on catalyst stability was reported by the authors. Weiß et al. report the inhibiting influence of catalyst reduction by H_2 crossover at cycling to the zero-current potential.⁶ Furthermore, Kwan et al. stress the importance of being able to translate RDE results into technically relevant CCM applications.⁷ Additionally, the importance of complementary analysis of catalyst dissolution (e. g. by ICP-MS, EQCM etc.) was stressed by several research groups as the observed performance degradation or improvements can be due to several superimposed effects.^{8–10}

Here we report detailed investigations and optimization of ADTs previously suggested by our group and showcase their wide

application range and functionality.² Thin-film model catalysts were employed to sufficiently separate the influences of the ADT protocols on anode catalyst degradation from other processes such as PTL or current collector oxidation as well as membrane thinning. To explore and better deconvolute the detailed effects of the ADT protocol on catalyst stability, a monometallic IrOx catalyst was chosen over any, possibly more reactive, yet more complex multi-metallic catalyst system. Translation of thin film results to catalyst coated membranes (CCMs) of single PEM electrolyzer cells showcases the successful implementation and usefulness of the ADT protocols in PEM electrolyzer degradation research.

We propose and analyze a *transient ADT* protocol that comprised of potential square-wave cycles between 0.05 V_{RHE} and various upper turning potentials E_{up} . Depending on the upper potential the protocol will be denoted as ADT- xV with xV corresponding to the upper turning potential. *Static* reference measurements were conducted as CAs at the same potentials as E_{up} . Additionally, chronopotentiometry (CP) was measured for 95 h to represent typical *static* long-term stability tests. Samples in this study are denoted as IrOx with the suffixes *-ap* (as prepared), *-ADT- xV* , *-CA- xV* and *-CP* respectively. Supplemental CCM measurements are denoted as CCM- followed by the one of the above-mentioned suffixes or by *-PC* for an additional power cycling protocol which mimics studies by Rakousky et al. and Weiß et al.^{5,6} The corresponding protocols and catalyst preparation are described in the experimental section and supporting information.

Experimental

In order to focus on protocol development a simple IrOx thin film was chosen as reference catalyst for all RDE measurements. In CCM measurements Elyst Ir75 0480 (Umicore) was used as anode catalyst, which was also measured in RDE for better comparison. For each catalyst at least three individual measurements were conducted on separately synthesized samples.

The reference IrOx thin film was deposited on a 10 mm polished Ti disc as described in previous publications and in the SI.¹¹ CCMs were produced in-house on Nafion NR-212 and spray coated as described in the supporting information. The Umicore-RDE measurements were conducted on a gold substrate RDE and are described in the supporting information in detail.

*Electrochemical Society Member.

^zE-mail: pstrasser@tu-berlin.de

Different electrochemical protocols were used to investigate the influence of test type (*transient* vs *static*) and potential. First, the *transient ADT* suggested in our previous publication was tested² but with 15,000 square-wave cycles resulting in 25 h *ADT* runtime and various upper turning potentials E_{up} ($= 1.4, 1.6, 1.8$ or $2.0 V_{RHE}$) with holding times of 3 s each. *Static* reference measurements were conducted as *CAs* at the same potentials for 25 h to mimic the *ADT* duration. A long-term stability reference *CP* was measured at 10 mA cm^{-2} for 95 h. The corresponding protocols are described in the supporting information. Additionally, considerations on fast current response three-electrode cell design are given in the supporting information as well (Figs. S14–S16 (available online at stacks.iop.org/JES/168/034508/mmedia)). All RDE measurements were conducted in $0.05 \text{ M H}_2\text{SO}_4$ at room temperature with a VSP Potentiostat (BioLogic, France), whereas CCM measurements were conducted on a Greenlight ETS electrolysis test station (Greenlight, Canada) at 80°C and 1 bar balanced pressure (anode and cathode at the same pressure) with DI-water flowing at the anode side with $5 \text{ ml min}^{-1} \text{ cm}^{-2}$.

Catalyst degradation was followed electrochemically through assessment of OER performance, redox activity and surface charge development in CVs as well as with potentiostatic electrochemical impedance spectroscopy (PEIS). Subsequent to each protocol, the electrolyte was analyzed for dissolved species by ICP-MS (ICAP Q ICP-MS, Thermo Fischer). Catalyst surface, phase and composition were investigated by XRD (D8 Advance, Bruker) and SEM-EDX (JEOL 7401 F with Quantax 400 detector) before and after testing. The extensive analysis allows a comprehensive deduction of the degradation phenomena induced by static and transient operation. Further information on experimental procedures can be found in the SI.

Results and Discussion

Impact of the novel proposed ADT protocol.—The summarized catalyst properties of *IrOx-ap* are shown in Fig. S1 to highlight the starting point of each of the applied tests. The reference catalyst is characterized by a smooth and homogeneous surface with typical redox features of thermally prepared IrO_2 in the cyclic voltammogram (CV)¹² and short-range IrO_2 rutile motifs as identified in TEM-SAED (Fig. S1c).

Initially, *ADT-1.4 V* was tested as suggested in our previous publication ($0.05\text{--}1.4 V_{RHE}$, 15,000 cycles)² with the respective characteristics presented in Fig. S2. The catalyst underwent severe changes within the first 2,500–5,000 cycles of the *ADT* resulting in increased electrochemically active surface area and cell resistance

concomitant with a slight decrease in specific OER performance (20% loss) in the later cycles. The latter is in line with observations on modified RDE measurements with CCMs¹³ and indicates actual catalyst degradation alongside the resistance increase. After the first 2,500 cycles the CV shape resembled that of electrochemically oxidized iridium and no longer that of thermally prepared IrOx ¹² in line with literature highlighting the electrooxidation of iridium in similar potential ranges.¹⁴ Constant values of the total anodic charge (Q_{anodic}) in later cycles indicate a stable electrochemically accessible area. The current densities are large when switching potentials between 0.05 and $1.4 V_{RHE}$ due to double layer capacitance charging and fast redox processes. This current, however, decreases within the first second to values below $\pm 0.1 \text{ mA cm}^{-2}$.

As reflected by the change in CV shape, *ADT-1.4 V* predominantly led to surface oxidation, increased anodic charge (Q_{anodic}) and cell resistance. Since the thin-film catalyst covers the whole electrode area, support oxidation seems to be an unlikely explanation for the resistance increase. More likely explanations are that the electrochemically formed IrOx on the catalyst surface generated additional contact resistances at the interface to the thermally prepared oxide underneath, or displayed metal-semiconductor transitions typical for Ir oxides annealed at low temperatures.¹⁵

Extended transient ADT and complementary Static OER tests.—In order to further investigate the *ADT*'s impact on catalyst stability, the test range was extended to $E_{up} = 1.6, 1.8$ and $2.0 V_{RHE}$. Comparative *static CA* tests at the same potentials were run for the same duration. Additionally an extended *static* test was run for 95 h to correlate degradation in the *transient ADT*s to different *static* runtimes. First, we turn to the physicochemical changes induced by the investigated protocols.

The X-ray diffraction patterns of *IrOx* developed distinctly different depending on the applied protocol. All *ADT* protocols except for *ADT-2.0 V* led to increased crystallinity when compared to *IrOx-ap* (Fig. S3a). *CA* measurements did not reveal any changes in the diffraction patterns regardless of the applied potential (see Fig. S3b). Only extended *static* measurement for 95 h (*IrOx-CP*) resulted in IrO_2 reflexes comparable to those on *IrOx-ADT-1.6 V*.

Akin to the XRD patterns, CVs of all *IrOx-CA* samples look alike and unaffected by the test while the *IrOx-ADT-CVs* show a distinct progression of changes with increasing applied potential (cf. Fig. 1). *IrOx-ADT-CVs* are dominated by the transition from the initial thermal IrOx shape towards a feature-rich shape resembling electrochemically oxidized IrOx with three redox features *a*, *b* and *c* (cf. Fig. 1a).¹² The main redox feature *b* at ca. $0.95 V_{RHE}$ represents the

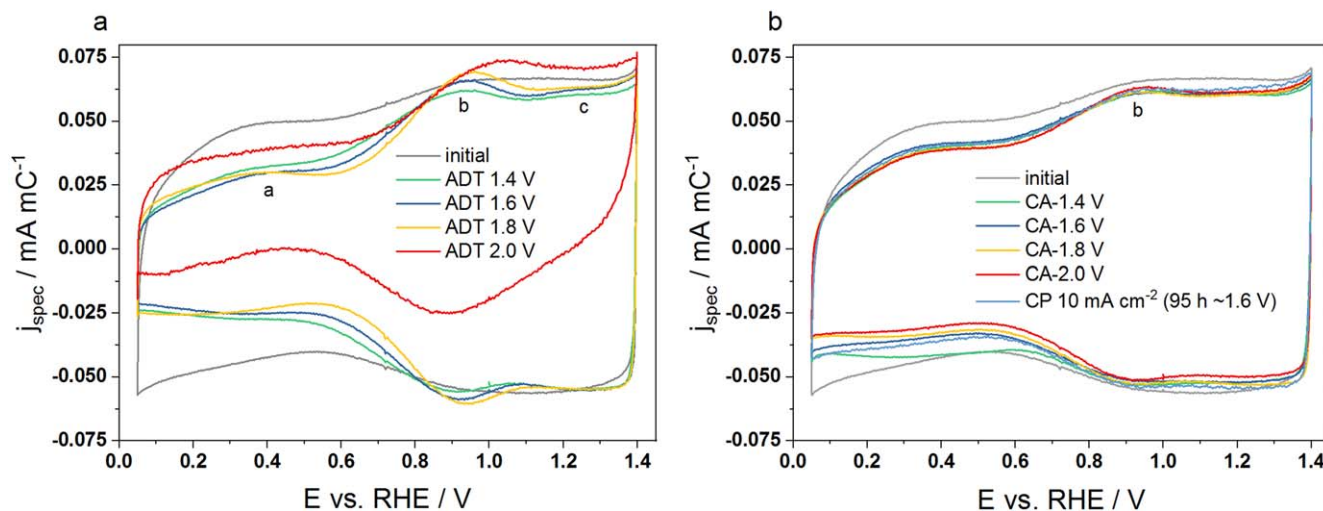


Figure 1. Charge normalized CVs of all investigated *IrOx* catalysts showing the final CV after (a) *transient* operation in the *ADT* protocols as well as (b) *static* operation in *CAs* or extended *CP*. The initial CVs of all catalysts were virtually identical and are represented by an exemplary CV given in grey. Scan rate 50 mV s^{-1} , $0.05 \text{ M H}_2\text{SO}_4$.

transition of $\text{Ir}^{\text{III}+}$ to $\text{Ir}^{\text{IV}+}$.¹⁴ With increasing E_{up} , a larger amount of redox active Ir and stabilization of reduced Ir states (cf. growing redox feature *b*, Fig. 1a) was observed for the ADTs. Strikingly, transient operation in ADT-1.4 V already resulted in stronger change than the most severe static protocol CA-2.0 V (Fig. 1b). This suggests that static operation (CA/CP) formed a very similar active Ir species and electrochemically active surface structure regardless of potential and test duration, whereas the transient ADT protocols resulted in distinct surface structures. A more detailed analysis of the CVs is given in the supporting information. When following the change of Q_{anodic} and cell resistance R throughout the protocols, R did not show a large dependence on the applied potential or protocol except for ADT-1.4 V (see Fig. S4a,b). Q_{anodic} decreased with increasing applied potential for all tests, however with a much stronger effect in the ADT-protocols (see Figs. S4c, S4d). SEM images did not reveal any changes in the morphology of the static samples even after prolonged operation for 95 h, while severe film damage was observed on IrOx-ADT-1.8 V and almost complete destruction of IrOx-ADT-2.0 V (cf. Figs. S5, S6). In all these properties, IrOx-ADT-1.6 V closely resembled the oxide formed after static tests (CA/CP) while resulting in enhanced degradation.

The electrochemical steady state activity at an overpotential of $\eta = 300$ mV (1.53 V_{RHE}) was measured during the initial and final OER scans. To compare the effect of the applied protocols on OER performance degradation, the remaining activity in the final scan was calculated as fraction of the initial activity, which is shown in Figs. 2a and 2b for mass-based and specific activity. An almost linear relationship between remaining activity and upper turning potential was found, where even the softest transient protocol ADT-1.4 V resulted in similar mass activity loss as obtained for the hardest static protocol CA-2.0 V. The increased mass activity of IrOx-CA-1.4 V and -1.6 V is likely due to the initial formation of an activated surface layer with larger electrochemically accessible surface area. It should be noted that extended static operation did not lead to strongly increased degradation (cf. IrOx-CA-1.6 V vs IrOx-CP; 25 h vs 95 h). The remaining specific activity of ADT-1.6 V and ADT-1.8 V appeared similar despite the increased physical layer damage observed on IrOx-ADT-1.8 V (see Fig. S5g) speaking in favor of additional catalyst degradation processes being present on the latter. Literature on thinning through electropolishing of Ir reports applied positive potentials of several volts and therefore is an unlikely mechanism here.¹⁶ Nevertheless, it seems possible that the observed increase in porosity marks the beginning of similar processes, e.g. through the recently observed formation of volatile IrO₃ species.¹⁷ Film rupturing by recurring sudden bubble formation at the applied high current densities and/or high potentials appears plausible too.^{18,19} Similarly, the specific activity of IrOx-ADT-2.0 V shows that, even though critically damaged, the remaining iridium retains a relatively high portion of its specific OER activity while the overall performance almost diminished. Strikingly, the ADT protocols give much higher reproducibility over the CA protocols (indicated by the significantly lower standard deviation of individual measurements; cf. error bars in Fig. 2).

Correlations between the observed activity loss and possible catalyst layer degradation were investigated by SEM-EDX analysis of the electrodes (Fig. 2c) and ICP-MS measurements of the electrolytes (Fig. 2d). The Ir/Ti ratio obtained by SEM-EDX acts as metric of the remaining layer thickness (see SI). This already indicated the more severe impact of transient over static operation with ADT-1.4 V resulting in similar catalyst loss as CA-2.0 V and CP. Complementary ICP-MS measurements completed this picture revealing significantly increased dissolution rates (Fig. 2d) for ADT measurements with an 11-fold increase of Ir dissolution during ADT-2.0 V vs that of CA-2.0 V. It should be noted, that the dissolution rates presented here were averaged over the total test duration and give no information about the dissolution rate gradient especially throughout the static experiments.

In order to elucidate the governing effects of the observed degradation, we compare the maximum anodic geometric current

densities during all protocols in Table I (see also Fig. S7 and S8). Current densities scaled with increasing potential independent of the protocol used. However, ADTs subject the catalyst to distinctly higher currents than the CAs at equal potentials because the former are superimposed with capacitive currents and do not allow for sufficient equilibration time per cycle. Interestingly, ADT-1.8 V and CA-1.8 V result in very similar current densities but dramatically different catalyst degradation. It follows that the accelerated degradation of ADT protocols cannot entirely be an effect of the applied current density. The electrode potential on the other hand, clearly influences the degree of degradation. On the -CA samples severe performance degradation could only be observed at $E_{\text{up}} > 1.8 V_{\text{RHE}}$, which is in agreement with the observation of volatile Ir compounds becoming favorable above those potentials.¹⁷ Additionally, the total Ir dissolution of IrOx-CP (95 h, 10 mA cm^{-2} , $\sim 1.6 V_{\text{RHE}}$) is slightly smaller when compared to IrOx-CA-1.6 V (25 h, 1.6 V_{RHE}), which suggests prolonged static measurements to be less destructive on the catalyst layer. The marginally larger dissolution rate of IrOx-CA-1.6 V over IrOx-CP implies a dissolution rate gradient that slowly levels out during constant operation. The latter is in line with observations from Geiger et al. and Alia et al., who found little impact of CAs longer than 13.5 h for initial stability tests.^{3,15} A plausible explanation for the increased degradation in our ADTs over the potential cycling experiments of Alia et al. is the lower turning potential of 0.05 V_{RHE} in our vs 1.4 V_{RHE} in the latter study.⁴ While the exact OER mechanism is subject to discussion, all recent works assume several iridium oxidation state changes to be involved, most commonly also an $\text{Ir}^{\text{III}+}$ state.^{17,20-22} Hence, forcing a majority of the catalyst layer through those oxidation state changes during transient protocols like the ADT proposed here is most likely the reason for the observed increased degradation over static OER operation where these changes happen at the electrochemically active catalyst surface only. We believe that this is the crucial difference between the low-impact cycling protocols observed by Alia et al. and the ones presented here.

ADT protocol validation for PEM-electrolysis.—To check the validity of our above conclusions and test the applicability of the proposed ADT to full single cell PEM electrolyzers, CCMs were subjected to the three following protocols: (i) 24 h operation at a constant potential of 1.75 V (CCM-CA); (ii) a 24 h power cycling (PC) protocol between 0 A cm^{-2} and a potential of 1.75 V, wherein each set point was held for 60 s (CCM-PC); (iii) the accelerated degradation test (CCM-ADT) protocol was carried out for 15,000 cycles between 0 V and 1.75 V with 3 s at each potential. 1.75 V were chosen to compare the ADT to a cycling protocol that was mentioned in a 3M talk at the ICE 2017 conference and give it industry relevance.²³ The power cycling protocol was chosen as additional reference in accordance with recent studies by Rakousky et al.⁵ and Weiß et al.²⁴ Figure 3 depicts the current-voltage profiles vs time for all three protocols as well as the polarization curve development during CCM-ADT.

Mass-based polarization curves of CCM-ADT are depicted in Fig. S9 with an inset zoomed on the low current region. The latter shows a strong impact of the ADT on performance on the kinetic region. As described in the literature,²⁵ transport losses by proton conductivity set in early in the kinetic region, too, and could be one reason for the observed performance loss on CCM-ADT. For example, a change in catalyst surface area or catalyst-ionomer interaction could have an impact on proton transport. Increased contact resistance was observed during PEIS measurements on CCM-ADT (see Fig. S10). Most likely, those were caused by degradation of the TiO₂ support or oxidation of the Ti felt PTL,²⁶ which, in turn, could affect proton conductivity or interparticle connection. The applied low potentials of the ADT could have similar or even more severe effects than the H₂ crossover induced reduction of catalyst and/or support observed by Weiß et al.²⁴ The overall shape of the Nyquist impedance (see Fig. S10) remained unchanged, indicating no additional mass-

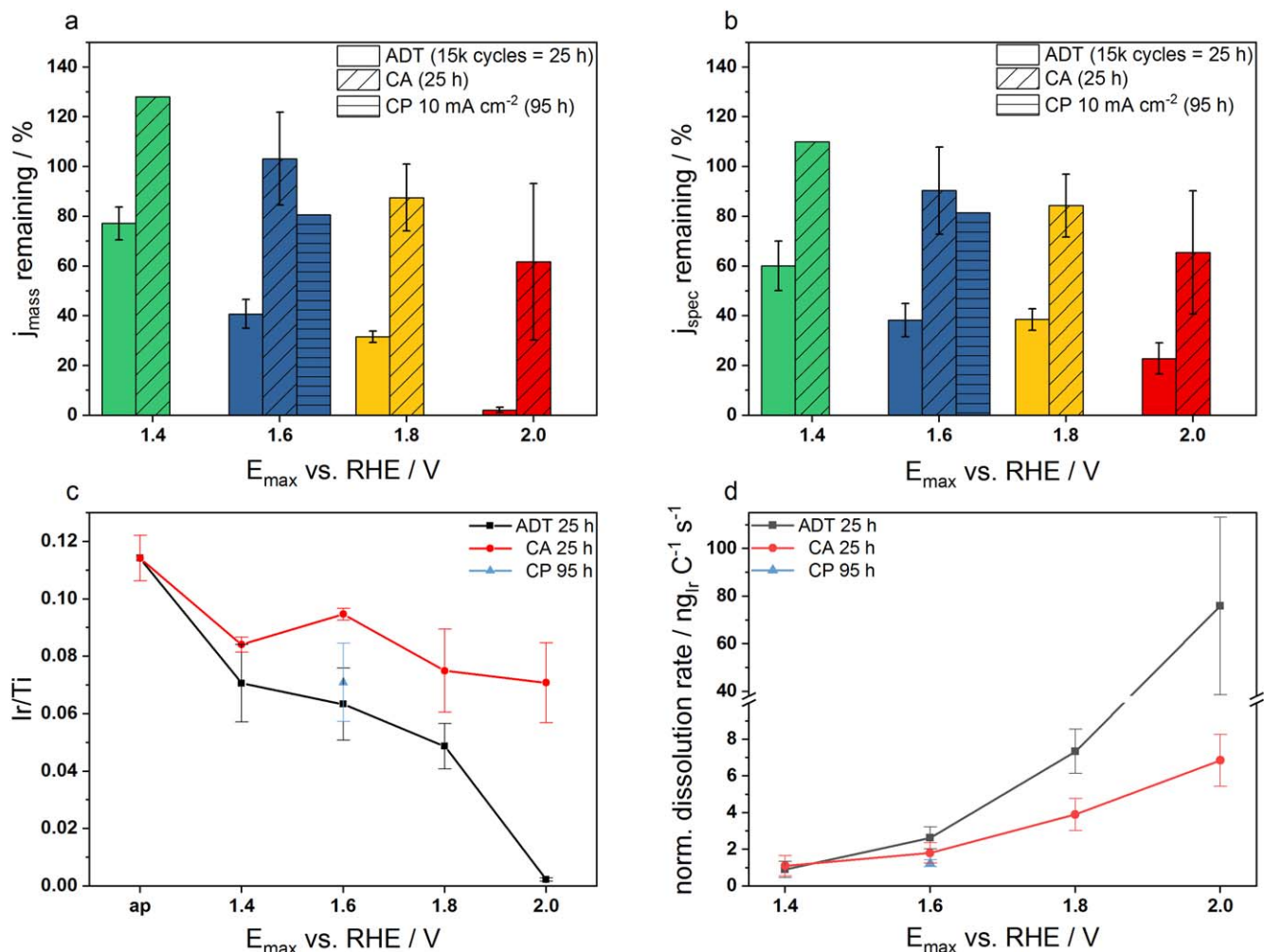


Figure 2. Catalyst degradation assessment. Remaining (a) mass and (b) specific activity of the -ADT and -CA samples at $1.53 V_{\text{RHE}}$. Due to the minimal activity loss after 25 h at $1.6 V_{\text{RHE}}$ the remaining activity after 95 h (IrOx-CP) was investigated as well. Catalyst loss was followed by (c) SEM-EDX measurement in form of the detected Ir/Ti ratio as well as by ICP-MS measurement of the dissolved species in the electrolyte, which were used to calculate the (d) charge normalized dissolution rates obtained during each of the protocols. Note the break in the y-axis of (d) due to significantly increased dissolution on ADT-2.0 V samples. The error bars in all subfigures represent the standard deviation of at least three independent measurements.

Table I. Anodic geometric current densities obtained during the ADT and CA protocols.

E_{\max} vs RHE/V	$j_{\text{geo ADT-protocols}}/\text{mA cm}^{-2}$	$j_{\text{geo CA-protocols}}/\text{mA cm}^{-2}$
1.4	0.05	0.02
1.6	10	5
1.8	30	30
2.0	60	40

transport resistances. A low, but most importantly, constant value for H_2 crossover during all three protocols was taken as indicator for the absence of membrane thinning. The latter was confirmed by SEM top-view and cross-section measurements that also showed no significant changes in the catalyst layer (see Fig. S11–S13).

The overall performance impact of the three applied protocols is compared in Fig. 4a and referenced to the ADT-RDE results in Fig. 4b.

The impact of *transient* fast potential cycling ADTs vs *static* CAs is lower in single cell PEM measurements than in the RDE study. The higher temperatures of CCM vs RDE tests (80°C vs $\sim 25^\circ\text{C}$) and higher loadings in CCMs may very well play a role here. Nevertheless, a significant increase of mass-activity losses was observed when comparing *transient* to *static* CCM measurements

at the same potential. For sake of better comparison, ADT-1.6 V was also measured with the Umicore catalyst used for the anodes of the CCM measurements. The resulting performance degradation is shown in light blue in Fig. 4b) while CVs are shown in Fig. S17. A similar degradation to ADT-1.6 V was observed, supporting the conclusions presented above. In line with data from Rakousky et al.⁵ an activity improvement was observed during the power cycling protocol on CCM-PC. Comparing the RDE- and CCM-ADT results suggest that degradation trends obtained by such a protocol in simplified RDE studies allow meaningful deductions for catalyst stability in PEM water electrolysis applications furthermore reducing research efforts and expenses.

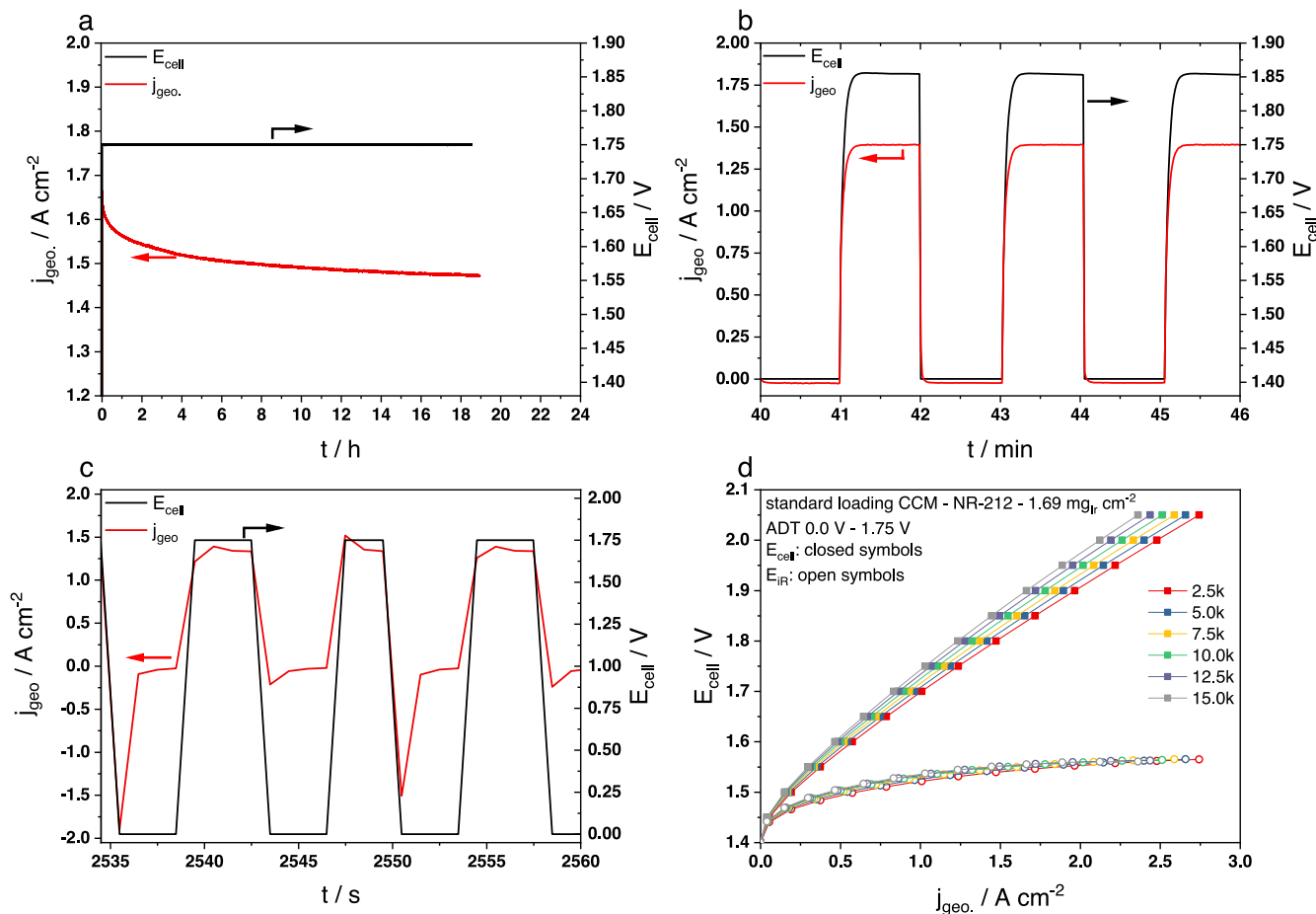


Figure 3. CCM degradation protocols summary. All measurements were conducted at 80 °C and with an anodic feed water flow of 0.05 l min⁻¹. All CCMs had an anode weight loading of 1.69 mg_{Ir} cm⁻². Current voltage profiles of (a) CCM-CA, (b) CCM-PC and (c) CCM-ADT. Subfigure (d) presents the polarization curves recorded on CCM-ADT after the corresponding cycles indicated in the figure key.

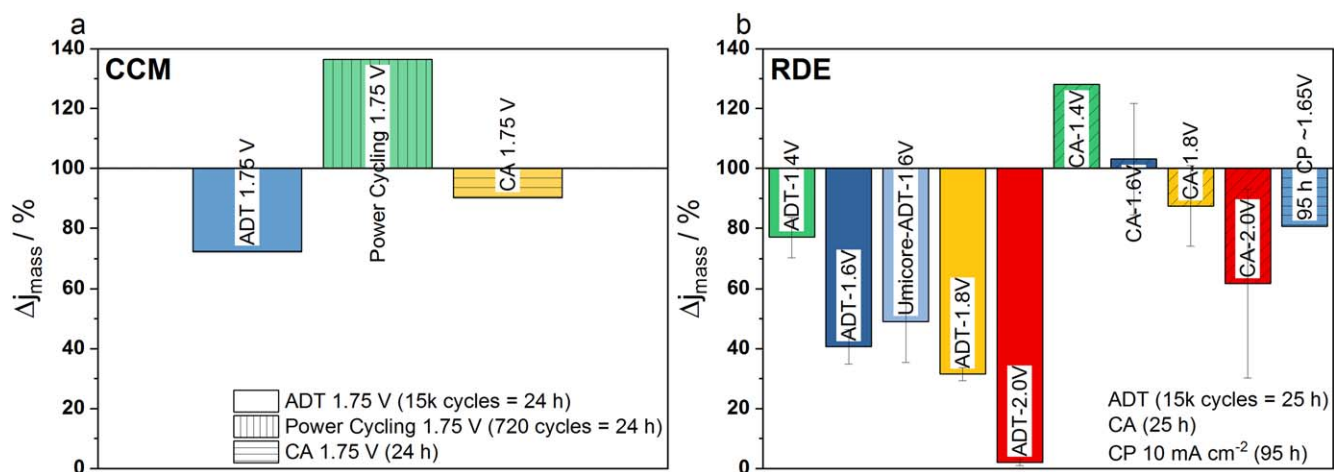


Figure 4. Comparison of ADT in (a) PEM electrolysis operation vs (b) RDE study with error bars corresponding to the standard deviation of at least three measurements. Relative mass activity loss vs applied protocol. *Umicore-ADT-1.6 V* in (b) represents comparative measurements of the CCM anode catalyst in an RDE setups. For details see supporting information.

Conclusions

In this study, a strong electrode potential dependence of catalyst dissolution was observed, which could be significantly enhanced by applying *transient ADT* protocols instead of *static CA* or *CP* protocols in, both, RDE and CCM tests. However, additional physical catalyst damage was observed on *IrOx-ADT* samples

subjected to potentials ≥ 1.8 V_{RHE} while physicochemical catalyst properties of *IrOx-ADT-1.6 V* developed analogous to *static* tests (conventionally used in OER stability tests). Hence, in order to mimic dissolution during static loads at significantly shorter test duration, we suggest *ADT-1.6 V* as new standard accelerated degradation test. 15,000 cycles (corresponding to 25 h of operation) resulted in a 3-fold increased Ir dissolution rate and 5-fold increased

OER performance loss in $\frac{1}{4}$ of the test duration when compared to *IrOx-CP* (10 mA cm^{-2} , 95 h, ca. $1.65 \text{ V}_{\text{RHE}}$). The observed degradation of *IrOx-ADT-1.6 V* should correspond to even longer *static* operation, clearly proving the advantage of *transient* operation for enhanced catalyst degradation studies. Forcing the catalyst to cycle through oxidation states that are thought to be involved in the OER is plausibly responsible for the enhanced degradation of the *ADT*. Adaptions with different lower turning potentials would be worth additional studies especially for the application to oxide-supported catalysts, where the support could become reduced at too cathodic potentials. We assume that the degradation effect should be similar as long as the potential range straddles the $\text{Ir}^{\text{III+}}/\text{Ir}^{\text{IV+}}$ redox peak but other issues such as O_2 bubble removal may arise. Furthermore, *static* constant current or constant potential stability measurements of less than 24 h have proven to be insufficient to test catalyst stability relevant for PEM electrolysis applications. Our study provides a powerful tool to researchers in the area of renewable energies and proves that a knowledge-driven approach such as taken in the development of this protocol⁵ can deliver significant advances for the scientific community. The *ADT*'s reproducibility (cf. Fig. 2) and applicability to both, RDE and CCM tests (cf. Fig. 4), add new significance to stability test results in OER research.

Acknowledgments

C.S. is grateful to Dr. Stefanie Kühn for the TEM-SAED measurement of *IrOx-ap* and to Ms. Claudia Kuntz from the Institute of Applied Geosciences at TU Berlin for measuring ICP-MS of the electrolyte samples. Funding through DFG Projekt „Iridium“ (DFG - Konsortium STR 596/11-1) is gratefully acknowledged.

ORCID

Camillo Spöri  <https://orcid.org/0000-0002-6071-4983>

Matthias Kroschel  <https://orcid.org/0000-0003-3321-8498>

Peter Strasser  <https://orcid.org/0000-0002-3884-436X>

References

- C. Rozain, E. Mayousse, N. Guillet, and P. Millet, *Appl. Catalysis B*, **182**, 123 (2016).
- C. Spöri, J. T. H. Kwan, A. Bonakdarpour, D. P. Wilkinson, and P. Strasser, *Angew. Chem. Int. Ed.*, **56**, 5994 (2017).
- S. M. Alia, B. Rasimick, C. Ngo, K. C. Neyerlin, S. S. Kocha, S. Pylypenko, H. Xu, and B. S. Pivovar, *J. Electrochem. Soc.*, **163**, F3105 (2016).
- S. M. Alia and G. C. Anderson, *J. Electrochem. Soc.*, **166**, F282 (2019).
- C. Rakousky, U. Reimer, K. Wippermann, S. Kuhri, M. Carmo, W. Lueke, and D. Stolten, *J. Power Sources*, **342**, 38 (2017).
- A. Weiß, A. Siebel, M. Bernt, and H. A. Gasteiger, *Meeting Abstracts*, **MA2018-02**, 1606 (2018).
- J. T. H. Kwan, A. Bonakdarpour, G. Afonso, and D. P. Wilkinson, *Electrochim. Acta*, **258**, 208-219 (2017).
- R. Frydendal, E. A. Paoli, B. P. Knudsen, B. Wickman, P. Malacrida, I. E. L. Stephens, and I. Chorkendorff, *Chem. Electro. Chem.*, **1**, 2075-2081 (2014).
- S. Geiger, O. Kasian, A. M. Mingers, S. S. Nicley, K. Haenen, K. J. J. Mayrhofer, and S. Cherevko, *Chem. Sus. Chem.*, **10**, 4140-4143 (2017).
- C. Rakousky, G. P. Keeley, K. Wippermann, M. Carmo, and D. Stolten, *Electrochim. Acta*, **278**, 324 (2018).
- C. Spöri, P. Brioso, H. N. Nong, T. Reier, A. Billard, S. Kühn, D. Teschner, and P. Strasser, *ACS Catal.*, **9**, 6653 (2019).
- L. Quattara, S. Fierro, O. Frey, M. Koudelka, and C. Cominellis, *J. Appl. Electrochem.*, **39**, 1361 (2009).
- M. Kroschel, A. Bonakdarpour, J. T. H. Kwan, P. Strasser, and D. P. Wilkinson, *Electrochim. Acta*, **317**, 722 (2019).
- T. Reier, M. Oezaslan, and P. Strasser, *ACS Catal.*, **2**, 1765 (2012).
- S. Geiger, O. Kasian, B. R. Shrestha, A. M. Mingers, K. J. J. Mayrhofer, and S. Cherevko, *J. Electrochem. Soc.*, **163**, F3132 (2016).
- L. E. Murr, *J. Less-Common Met.*, **34**, 177 (1974).
- O. Kasian, J. P. Grote, S. Geiger, S. Cherevko, and K. J. J. Mayrhofer, *Angew. Chem. Int. Ed. Engl.*, **57**, 2488 (2018).
- A. R. Zeradjanin, A. A. Topalov, Q. Van Overmeere, S. Cherevko, X. X. Chen, E. Ventosa, W. Schuhmann, and K. J. J. Mayrhofer, *RSC Adv.*, **4**, 9579 (2014).
- A. Hartig-Weiss, M. F. Tovini, H. A. Gasteiger, and H. A. El-Sayed, *ACS Appl. Energy Mater.*, **3**, 10323 (2020).
- T. Binnering, R. Mohamed, K. Waltar, E. Fabbri, P. Levecque, R. Kotz, and T. J. Schmidt, *Sci. Rep.*, **5**, 12167 (2015).
- T. Reier, H. N. Nong, D. Teschner, R. Schlögl, and P. Strasser, *Adv. Energy Mater.*, **7**, 1601275 (2017).
- H. N. Nong et al., *Nat. Catal.*, **1**, 841 (2018).
- K. Lewinski, F. Sun, S. Luopa, J. Park, R. Masel, and L. Nereng, "Operation of low-temp electrolyzers at very high current densities: a pipe dream or an opportunity?" *1st International Conference on Electrolysis*, Copenhagen (2017).
- A. Weiß, M. Bernt, A. Siebel, P. J. Rheinländer, and H. A. Gasteiger, *Meeting Abstracts*, **MA2017-02**, 1648 (2017).
- M. Bernt and H. A. Gasteiger, *J. Electrochem. Soc.*, **163**, F3179 (2016).
- C. Rakousky, U. Reimer, K. Wippermann, M. Carmo, W. Lueke, and D. Stolten, *J. Power Sources*, **326**, 120 (2016).